HHS Public Access

Author manuscript

Oncogene. Author manuscript; available in PMC 2017 March 31.

Published in final edited form as:

Oncogene. 2017 March 30; 36(13): 1887–1898. doi:10.1038/onc.2016.359.

The interaction between acetylation and serine-574 phosphorylation regulates the apoptotic function of FOXO3

Z Li[1], **B Bridges**[2], **J Olson**[1], and **SA Weinman**[1,2]

[1]Department of Internal Medicine, University of Kansas Medical Center, Kansas City, KS, USA

[2]Liver Center, University of Kansas Medical Center, Kansas City, KS, USA

Abstract

The multispecific transcription factor and tumor suppressor FOXO3 is an important mediator of apoptosis, but the mechanisms that control its proapoptotic function are poorly understood. There has long been evidence that acetylation promotes FOXO3-driven apoptosis and recently a specific JNK (c-Jun N-terminal kinase)-dependent S574 phosphorylated form (p-FOXO3) has been shown to be specifically apoptotic. This study examined whether acetylation and S574 phosphorylation act independently or in concert to regulate the apoptotic function of FOXO3. We observed that both sirtuins 1 and 7 (SIRT1 and SIRT7) are able to deacetylate FOXO3 *in vitro* and *in vivo*, and that lipopolysaccharide (LPS) treatment of THP-1 monocytes induced a rapid increase of FOXO3 acetylation, partly by suppression of SIRT1 and SIRT7. Acetylation was required for S574 phosphorylation and cellular apoptosis. Deacetylation of FOXO3 by SIRT activation or SIRT1 or SIRT7 overexpression prevented its S574 phosphorylation and blocked apoptosis in response to LPS. We also found that acetylated FOXO3 preferentially bound JNK1, and a mutant FOXO3 lacking four known acetylation sites (K242, 259, 290 and 569R) abolished JNK1 binding and failed to induce apoptosis. This interplay of acetylation and phosphorylation also regulated cell death in primary human peripheral blood monocytes (PBMs). PBMs isolated from alcoholic hepatitis patients had high expression of SIRT1 and SIRT7 and failed to induce p-FOXO3 and apoptosis in response to LPS. PBMs from healthy controls had lower SIRT1 and SIRT7 and readily formed p-FOXO3 and underwent apoptosis when similarly treated. These results reveal that acetylation is permissive for generation of the apoptotic form of FOXO3 and the activity of SIRT1 and particularly SIRT7 regulate this process *in vivo*, allowing control of monocyte apoptosis in response to LPS.

INTRODUCTION

FOXO3 is a transcription factor that is responsible for multiple transcriptional programs including cell-cycle arrest,[1] DNA repair,[2] antioxidant stress responses,[3] apoptosis,[4] autophagy[5] and aging.[6] It is a well-established mediator of cell death in cancer cells, is pivotal for the maintenance of organ homeostasis[7] and is frequently dysregulated in

Correspondence: Dr SA Weinman, Department of Internal Medicine, University of Kansas Medical Center, 3901 Rainbow Boulevard, Mailstop 1018, Kansas City 66160, KS, USA. sweinman@kumc.edu.

CONFLICT OF INTEREST

The authors declare no conflict of interest.

cancer.[8–10] FOXO3 promotes apoptosis by inducing the expression of death receptor ligands, including Fas ligand and tumor necrosis factor-related apoptosis-inducing ligand (TRAIL), as well as through induction of proapoptotic Bcl-2 family members, such as Bim, bNIP3 and Bcl-XL.[11] FOXO3 apoptosis is highly context dependent and largely effected by upstream enzymes. We recently identified a JNK (c-Jun N-terminal kinase)-dependent S574 phosphorylated form of FOXO3 (p-FOXO3) that selectively binds to proapoptotic promoters, acts as a transcriptional repressor of Bcl-2 and induces apoptosis in both hepatocytes and monocytes.[12] The formation of p-FOXO3, however, varied depending on the stimulus and the cell culture conditions and thus whether or not a given stimulus would reliably produce apoptosis could not be easily predicted. Previous work suggested that acetylation also has a role in regulating the apoptotic function of FOXO3 and deacetylation caused by sirtuin (SIRT) family deacetylases favored the antioxidant as opposed to the apoptotic function of FOXO3.[13]

SIRT or silent information regulator 2 (Sir2) proteins are nicotinamide adenine dinucleotide (NAD^+)-dependent deacetylases and ADP-ribosyl transferases. In mammals, seven SIRT proteins have been identified all sharing the NAD^+ binding and catalytic domain, but targeting different substrates.[14] SIRT proteins regulate a variety of processes including metabolism,[15,16] cell survival,[13,17,18] differentiation[19] and DNA repair,[20] mainly by deacetylating lysine residues on histones, transcription factors or coactivators. Well-recognized SIRT targets include SREBP-1C,[21] FOXO3,[22] p53[23] and p65.[24] SIRTs have critical roles in controlling stress resistance and apoptosis. SIRT1 deacetylates p53 and controls DNA damage-induced acetylation of p53, which in turn suppresses cell-cycle arrest and apoptosis.[25] Multiple SIRT family members have been reported to control FOXO3-dependent apoptosis through deacetylation of FOXO3.[13,17,22] Expression or activation of SIRT1, SIRT2, SIRT3 and SIRT5 all favored FOXO3's antioxidant phenotype, suggesting that acetylated FOXO3 is more apoptotic, whereas deacetylated FOXO3 is more antioxidant. The recent recognition that p-FOXO3 is critical for FOXO3-induced apoptosis[12] raises the question of whether acetylation affects FOXO3 apoptosis by an independent mechanism or by regulating the formation or function of p-FOXO3. In this study, we examined the relationships between FOXO3 acetylation, S574 phosphorylation and cellular apoptosis. We found that acetylation is required for apoptosis because it is necessary for p-FOXO3 formation. These data thus provide a new understanding of the link between acetylation and FOXO3-induced apoptosis.

RESULTS

FOXO3-dependent monocyte apoptosis requires FOXO3 acetylation

To examine the role of acetylation in lipopolysaccharide (LPS)-induced, FOXO3-dependent apoptosis, we treated THP-1 cells with 100 ng/ml LPS for 6 h and compared FOXO3 acetylation with the formation of p-FOXO3. LPS treatment resulted in the accumulation of p-FOXO3 and a global increase in protein acetylation (Figure 1a). Co-immunoprecipitation showed that LPS increased FOXO3 acetylation and this was apparent at 0.5 h, before the formation of p-FOXO3 (Figure 1b). To examine whether acetylation is required for p-FOXO3 formation, we treated cells with LPS in the presence of SIRT activators or a p300

inhibitor (C646). Figure 1c demonstrates that resveratrol (RSV), a well-known SIRT activator, and CAY10591, a more selective SIRT1 activator, both reduced FOXO3 acetylation and largely abolished p-FOXO3 formation. Inhibition of the acetyltransferase p300 had only minor effects on FOXO3 acetylation and phosphorylation (Figure 1c). The prevention of p-FOXO3 formation by SIRT activators occurred even though there was no effect on the activation of JNK, the upstream kinase responsible for FOXO3 phosphorylation.[12]

To determine if SIRT activators also block apoptosis, we measured TRAIL and Bcl-2 mRNA, increases and decreases of which, respectively, are necessary for p-FOXO3-triggered apoptosis.[12] SIRT activators completely abolished both the LPS-induced increase of TRAIL and the decrease of Bcl-2 mRNA and protein but had no effects on FOXO3 mRNA (Figures 1d and e). SIRT activators also blocked LPS-induced apoptosis pathway activation as evidenced by caspase-3/7 activity, poly (ADP-ribose) polymerase cleavage and formation of terminal deoxynucleotidyl transferase dUTP nick-end labeling (TUNEL)-positive cells (Figures 1e–g) and prevented the loss of cell viability after LPS. These data show that acetylation of FOXO3 is essential for p-FOXO3 formation and p-FOXO3-dependent apoptosis.

LPS induces acetylation of FOXO3 by targeting SIRT1 and SIRT7

FOXO3 acetylation levels are determined by the opposing actions of protein acetyltransferases and protein deacetylases, including members of the Sir2/Sirt family.[6] As the p300 inhibitor had only minor effects on FOXO3 acetylation, we focused on SIRT family proteins. LPS treatment resulted in decreases of both SIRT1 and SIRT7 protein levels (Figure 2a). For SIRT7 this change was reflected by decreased mRNA as well (Figure 2b). For SIRT1, however, mRNA levels actually increased, suggesting that SIRT1 is controlled by non-transcriptional mechanisms. We thus next measured SIRT protein stability in the presence of cycloheximide. As shown in Figure 2c, LPS decreased the half-life of SIRT1, SIRT2, SIRT6 and SIRT7. The proteasome inhibitor MG-132 increased the amount of SIRT1 and SIRT7 in the presence of LPS. Consistent with these observations, LPS treatment resulted in a progressive decrease of SIRT activity (Figure 2e). This decreased activity occurred in spite of increased or unchanged levels of the SIRT substrate NAD^+ (Figure 2f).

MAPKs trigger SIRT1 and SIRT7 degradation

The mitogen-activated protein kinase (MAPK) cascade is a key downstream pathway for LPS-induced signaling events[26] and has been implicated as a regulator of SIRT activity and stability.[27] We thus investigated whether MAPKs are involved in LPS-induced SIRT1 and SIRT7 downregulation. Both SP600125 (JNK inhibitor) and FR180204 (ERK inhibitor) diminished the decrease of SIRT1 and SIRT7 and the increase of p-FOXO3 after LPS (Figure 3a). To confirm these observations, we overexpressed variants of MAPKs and monitored SIRT1 and SIRT7 protein levels. JNK1, ERK1, ERK2 and p38 overexpression all decreased SIRT1, whereas only ERK1 and ERK2 decreased SIRT7 (Figures 3b–e). Similar results were observed from cells transfected with Flag-tagged MAPKs (Figure 3f). SIRT1 and SIRT7 were diffusely localized in the nucleus in untransfected cells. Overexpression of each of the MAPKs decreased the SIRT1 signal but only ERK1 and ERK2 decreased the

SIRT7 signal. Of note, the JNK inhibitor blocked the SIRT7 decrease but overexpression of JNK1 had no effect on SIRT7. Overexpression of p38 decreased SIRT7 but the p38 inhibitor had no effect, suggesting that p38 is not vital for the SIRT7 decrease during LPS treatment. Finally, we performed immunoprecipitation to examine protein–protein interactions between MAPKs and SIRT1/SIRT7. Each of the MAPKs directly bound to both SIRT1 and SIRT7 (Figure 3g).

SIRT7 deacetylates FOXO3

Multiple SIRT family members have been reported to deacetylate FOXO3.[13,18,28] We thus investigated whether SIRT7 deacetylates FOXO3 as well. We performed immunoprecipitation and found a direct interaction between these two proteins in THP-1 cells (Figure 4a). This prompted us to examine whether SIRT7 deacetylates FOXO3. HA-FOXO3 was expressed in HeLa cells and cells were treated with hydrogen peroxidase to induce acetylation of FOXO3.[13] We then purified this acetylated FOXO3 and incubated it *in vitro* with rSIRT7. As reported, hydrogen peroxidase induced acetylation of FOXO3 and it became deacetylated only after the simultaneous addition of rSIRT7 and NAD^+ (Figure 4b). To examine the role of SIRT7 in FOXO3 deacetylation, we knocked down SIRT7 in THP-1 cells that had been incubated with the class I and II histone deacetylase inhibitor trichostatin A (TSA) and measured FOXO3 acetylation. SIRT7 knockdown alone had no effect on FOXO3 acetylation. Treatment with TSA alone slightly increased FOXO3 acetylation and incubation of siSIRT7-treated cells with TSA led to a further increase in FOXO3 acetylation (Figure 4c). These results suggest that both SIRT7 and class I and II histone deacetylases contribute to FOXO3 deacetylation within cells.

SIRT1 and SIRT7 regulate p-FOXO3 formation and apoptosis

We next tested if SIRT1 and/or SIRT7 could block p-FOXO3 formation and apoptosis. HA-FOXO3 and Flag-JNK1 were co-transfected with either SIRT1 or SIRT7 and p-FOXO3 was measured by western blot. JNK1 decreased SIRT1 level and induced robust formation of p-FOXO3; restoring SIRT1 expression completely abolished p-FOXO3 formation (Figure 5a). Although JNK1 had no effect on SIRT7 level, SIRT7 overexpression similarly abolished p-FOXO3 formation (Figure 5b). To further confirm that SIRTs abolish p-FOXO3 formation through their enzyme activity, we incubated cells with the SIRT1 activator CAY10591. CAY10591 reduced p-FOXO3 protein level, but not as strikingly as SIRT1 overexpression. In contrast, a catalytically inactive SIRT7 mutant (H187Y) had no effect on JNK1-induced p-FOXO3 (Figure 5d). These data clearly suggest that SIRT1 and SIRT7 regulate p-FOXO3 through their deacetylase activity.

We next tested whether SIRT1 and SIRT7 could block LPS-induced apoptosis. We overexpressed SIRT1, SIRT7 and inactive SIRT7 H187Y in THP-1 cells by electroporation and treated with LPS. SIRT1 and SIRT7 significantly blocked LPS-induced acetylation of FOXO3 and p-FOXO3 formation, but SIRT7 H187Y had no effect on either process (Figure 5e). Furthermore, SIRT1 or SIRT7 completely blocked LPS-induced apoptosis as evidenced by cleaved poly (ADP-ribose) polymerase, caspase activity and TUNEL-positive cells (Figures 5f–h). Again, SIRT7 H187Y failed to block these processes. To evaluate whether endogenous SIRT1 or SIRT7 regulate p-FOXO3 and cell death, we treated THP-1 cells with

small interfering RNA (siRNA) targeting SIRT1 or SIRT7 for 72 h. SIRT1 knockdown resulted in a 1.5-fold increase of p-FOXO3, whereas SIRT7 knockdown resulted in sixfold increase of p-FOXO3 (Figure 5i), increased caspase activity (Figure 5j) and decreased cell viability (Figure 5k). These results demonstrate that SIRT7, but not SIRT1, is the major check point suppressing p-FOXO3-dependent cell death under resting conditions within THP-1 cells.

Acetylation of FOXO3 increases its interaction with JNK1

As JNK1 phosphorylates FOXO3 at S574,[12] allowing formation of the proapoptotic species, we tested whether FOXO3 acetylation is required for the JNK1–FOXO3 interaction. HeLa cells were co-transfected with HA-FOXO3 and Flag-JNK1 and were then treated with the deacetylase inhibitors TSA or sirtinol[29] or the SIRT activator RSV. We found that increasing FOXO3 acetylation with either TSA or sirtinol increased the binding of JNK1 to FOXO3, and the combination of the two had an additive effect (Figure 6a). In contrast, decreasing FOXO3 acetylation with RSV completely prevented JNK1 and FOXO3 binding (Figure 6a). These results strongly suggest that JNK1 preferentially binds to acetylated FOXO3. To further confirm that acetylation regulates the JNK1– FOXO3 interaction, we generated a FOXO3 mutant in which the four known acetylated lysines were replaced with arginines.[13,28] Two FOXO3-triple KR mutants with K242, K259 and K290 (3KR-A) or K242, K259 and K569 (3KR-B) mutated to arginine were also generated and tested. As shown in Figure 6b, the FOXO3-4KR mutant, but not the FOXO3-3KR mutants, had a greatly reduced level of acetylation. In addition, the interaction between JNK1 and FOXO3 proteins was nearly blocked in the 4KR mutant (Figure 6c). Thus, lysine acetylation of FOXO3 facilitated JNK1 docking onto FOXO3, but it was necessary to eliminate all four lysines to prevent JNK1 binding. Combinations of single, double or triple lysine substitutions were not sufficient to prevent binding.

To further examine whether acetylation effects p-FOXO3 formation and apoptosis, we transfected HA-FOXO3 or FOXO3 KR mutants into Huh7.5 cells and then treated cells with 50 mM EtOH overnight, a system previously shown to induce p-FOXO3.[12] The 4KR mutant was defective in p-FOXO3 formation (Figure 6d). Similar results were obtained in HeLa cells co-transfected with HA-FOXO3 and Flag-JNK1 (Figure 6e), demonstrating that FOXO3 acetylation regulates JNK1-dependent p-FOXO3 formation under multiple conditions. Finally, the 4KR mutant failed to induce apoptosis after JNK1 expression demonstrating the importance of this effect (Figures 6f and g).

Impairment of LPS-induced apoptosis in the monocytes of patients with alcoholic hepatitis

To investigate whether the SIRT–FOXO3–apoptosis axis might have a role in human disease, we examined peripheral blood monocytes from patients with alcoholic hepatitis (AH), an inflammatory disease in which monocytosis has a role in pathogenesis.[30] We isolated monocytes from healthy control (HCs) and patients with AH and measured LPS-induced apoptosis. The clinical features of the subjects included in this study are presented in Table 1. In control monocytes, LPS induced both caspase-3/7 activity and loss in cell viability. In contrast, LPS failed to increase caspase-3/7 activity or decrease viability in AH monocytes (Figures 7a and b). In HC monocytes, LPS induced an eightfold increase of p-

FOXO3, but this was greatly reduced in AH monocytes (Figures 7c and d). SIRT1 and SIRT7 mRNA and protein levels were significantly higher in patients with AH (Figures 7e and f), possibly explaining the failure of the AH monocytes to phosphorylate FOXO3 and undergo apoptosis. To test this hypothesis, cells were treated with the SIRT inhibitor sirtinol and then tested again for LPS effects (Figures 7g and h). In control monocytes, sirtinol had no effect on caspase-3/7 activity or viability after LPS. In AH monocytes, in contrast, sirtinol reversed the failure of LPS to increase the caspase-3/7 activity and decrease viability. These results suggest that high SIRT activity is the primary event leading to the lack of p-FOXO3 formation and apoptosis in peripheral blood monocytes from patients with AH.

DISCUSSION

In this study, we have shown that formation of the proapoptotic p-FOXO3 is regulated by the state of FOXO3 acetylation. The acetylated form preferentially interacts with JNK, which triggers FOXO3 phosphorylation at S574. At baseline, FOXO3 is maintained in a deacetylated state largely through the activity of the deacetylases SIRT1 and SIRT7. In THP-1 cells, LPS treatment activates MAPKs and induces acetylation of FOXO3 by targeting SIRT1 and SIRT7 for degradation. This downregulation of SIRT1 and SIRT7 is essential for JNK-dependent p-FOXO3 formation and apoptosis. In AH, a disease in which abnormally high monocyte and tissue macrophage numbers are present, we see elevated monocyte SIRT1 and SIRT7 levels, which prevent p-FOXO3 formation and cause a defect in the apoptotic response to LPS.

It has long been recognized that the function of FOXO3 is regulated by acetylation. Brunet *et al.*[13] identified five acetylated lysine residues (K242, K245, K271, K290 and K569), and acetylation of FOXO3 exerts an inhibitory effect on transactivation activity by reducing its DNA-binding activity.[11] Multiple SIRT proteins have been reported to deacetylate FOXO3 including SIRT1, SIRT2, SIRT3 and SIRT6.[13,17,22,31] Here we show that SIRT7 is also a FOXO3 deacetylase. We found that SIRT7 is able to reverse the hydrogen peroxide-induced acetylation of FOXO3, suggesting that SIRT7 may deacetylate FOXO3 at the same sites as SIRT1 *in vitro*. Although SIRT1 and SIRT7 share similar ability to deacetylate FOXO3, knockdown of these two proteins produced different effects, suggesting that SIRT7 is the more important control point for p-FOXO3 formation and apoptosis in THP-1 cells.

The mechanism by which the FOXO3 acetylation state controls p-FOXO3 formation is not fully known, but acetylation promotes the binding of FOXO3 to JNK1 and this interaction is necessary for S574 phosphorylation. The JNK1–FOXO3 binding interaction was reduced by substituting four of the acetylated lysines with arginine, but this effect required all four lysines to be modified and no combination of either single or double lysine substitutions blocked JNK1 binding or phosphorylation. This suggests that no one specific acetylation site is responsible for the effect. Once p-FOXO3 has formed, manipulating protein acetylation with SIRT activators no longer prevented apoptosis (data not shown). This indicates that acetylation of FOXO3 is necessary for its ability to be S574 phosphorylated, but not for the ability of p-FOXO3 to cause apoptosis.

It is noteworthy that the SIRT deacetylases are themselves dynamically regulated by LPS as well. SIRT activity drops after LPS stimulation of THP-1 cells. In the case of SIRT1, this is primarily via post-translational mechanisms leading to more rapid degradation, but for SIRT7 a combination of decreased transcription and decreased protein stability both have a role. SIRT1 contains several post-translational modification sites that regulate protein stability and enzyme activity.[32] We found that LPS treatment results in a significant decrease of SIRT activity, which does not correlate with SIRT1 and SIRT7 protein levels, suggesting that activity regulation occurs as well. It has been shown that oxidants/aldehydes covalently modify SIRT1, decreasing its enzymatic activity and promoting its degradation.[33] These effects may have a role in apoptosis. There are also several serine phosphorylation sites on SIRT1 (Ser27, Ser47, Ser659 and Ser661) that are regulated by various protein kinases,[34–36] and we were able to show that MAPKs directly interact with SIRTs and mediate their degradation. JNK1 has been shown to phosphorylate SIRT1 at those sites leading to proteasome-mediated degradation.[27,37] These findings show that a web of interactions controlling SIRT activity, MAPK activation and p-FOXO3 formation all have a role in LPS-triggered, FOXO3-dependent apoptosis in monocytes.

The ability of SIRTs to regulate FOXO3-dependent cell death raises the possibility that manipulating this system may have therapeutic implications. RSV, the well-known SIRT activator, is recognized as an antiapoptosis and anti-inflammatory compound that can have beneficial effects in various diseases including rheumatoid arthritis and type I diabetes.[38,39] However, not all diseases benefit from the activation of SIRT1, possibly owing to the fact that apoptosis can have either deleterious or beneficial consequences depending on the cell type and precise pathogenic mechanisms involved. The complexity of the role of apoptosis in disease progression is well illustrated by the case of AH in which alcohol consumption triggers an unusually prolonged and severe inflammatory response within the liver that ultimately leads to hepatocyte apoptosis.[40] Although hepatocyte apoptosis appears to be contributing to disease severity, proinflammatory hepatic macrophages also undergo apoptosis in response to alcohol,[41] and in this case, apoptosis serves as a mechanism that suppresses the inflammatory response. Our data show that peripheral blood monocytes from AH patients have high SIRT1 and SIRT7 activity, fail to form p-FOXO3 and have a defect of apoptosis in response to LPS. These results suggest that high SIRT levels in myeloid cells could be a primary event leading to enhanced inflammation.

This study demonstrates the interrelated nature of post-translational modifications of FOXO3 and explains how both acetylation and S574 phosphorylation control the apoptotic function of FOXO3. This finding reconciles the earlier understanding of acetylation control of apoptosis with the more recent finding that S574 phosphorylation specifically drives the FOXO3-dependent apoptosis. Further studies will be required to better understand how acetylation affects kinase binding and whether there are apoptotic effects of acetylation that are independent of p-FOXO3. Nonetheless, the understanding of the interplay between acetylation and specific phosphorylation in FOXO3 provides a new understanding of molecular mechanisms by which SIRT proteins regulate cell function and point to SIRT7 as a potentially important target for disease modification.

MATERIALS AND METHODS

Cell culture, plasmids and transfection

THP-1 cells were purchased from ATCC (Manassas, VA, USA) and maintained in RPMI-1640 medium (Invitrogen, Grand Island, NY, USA) containing 10% fetal bovine serum and 0.05 mM 2-mercaptoethanol. Huh7.5 cells (provided by Dr Charles Rice, Rockefeller University, New York, NY, USA) and HeLa cells (provided by Dr Robert A Davey, University of Texas-Medical Branch, Galveston, TX, USA) were maintained in Dulbecco's modified Eagle's medium (Invitrogen, Grand Island, NY, USA) containing 10% fetal bovine serum, 50 U/ml penicillin and 50 mg/ml streptomycin. Cells were transfected in the presence of serum-free medium (Opti-MEM; Invitrogen) by using X-tremeGENE HP DNA Transfection Reagent (Roche, Indianapolis, IN, USA) according to the manufacturer's instructions. pECE-HA-FOXO3, pCDNA3 Flag MKK7B2Jnk1a1, pCDNA3 Flag p38α, pFLAG-CMV-hErk1 and p3xFlag-CMV7-Erk2 were, respectively, provided by M Greenberg, RJ Davis and Melanie Cobb via Addgene (Cambridge, MA, USA). FOXO3 point mutations were generated by Q5 Site-Directed Mutagenesis Kit (New England BioLabs, Ipswich, MA, USA). For siRNA transfections, 1×10^6 cells were plated and cultured overnight. Thereafter, gene-specific siRNAs were transfected in the presence of Opti-MEM medium using X-tremeGENE siRNA Transfection Reagent (Roche) according to the manufacturer's instructions. siRNA targeting SIRT1 (SMARTpool: ON-TARGET plus human SIRT1 siRNA) and SIRT7 (SMARTpool: ON-TARGET plus human SIRT7 siRNA) were purchased from GE Dharmacon (Lafayette, CO, USA). For electroporation, 1×10^7 THP-1 cells were resuspended in 400 μl serum-free RPMI media and incubated with 10 μg DNA for 5 min on ice before being electroporated at 140 V and 1000 μF. Following electroporation, 600 μl complete RPMI medium was added to the cells, which were kept on ice for 15 min, and then grown in 5 ml media for 48 h.

Antibodies and chemicals

A custom p-FOXO3 rabbit polyclonal antibody was generated as described previously.[12] Anti-HA antibody (ab9110) was purchased from Abcam (Cambridge, MA, USA). Anti-FOXO3 (75D8), anti-acetylated-lysine (9441), anti-Bcl-2 (50D3), anti-TRAIL (C92B9), anti-SIRT1 (D1D7), anti-SIRT7 (D3K5A), anti-SAPK/JNK, p-SAPK/JNK (T183/Y185) and anti-poly (ADP-ribose) polymerase (9542) were purchased from Cell Signaling Technology (Boston, MA, USA). Anti-SIRT6 was purchased from Abnova (Walnut, CA, USA). Anti-GAPDH (FL-335) and anti-TRAIL (H-257) were purchased from Santa Cruz Biotechnology (Dallas, TX, USA). Anti-actin (AC-15), anti-SIRT2 and anti-Flag (M2) were purchased from Sigma-Aldrich (St Louis, MO, USA). RSV, TSA, C646 and sirtinol were purchased from Sigma-Aldrich. NAD^+ and CAY10591 were purchased from Cayman Chemical (Ann Arbor, MI, USA). rSIRT7 was purchased from SignalChem (Richmond, BC, Canada). SP600125 was purchased from Cell Signaling Technology. SB203580 was purchased from AdipoGen (San Diego, CA, USA). FR180204 was purchased from Calbiochem (Billerica, MA, USA). LPS from Escherichia coli O55:B5 was purchased from Enzo Life Science (Farmingdale, NY, USA).

Immunofluorescence

For indirect immunofluorescence, cells grown on coverslips were fixed with 4% paraformaldehyde and permeabilized in 0.2% Triton X-100. The coverslips were inverted and touched to 40 μl droplets of blocking buffer (4% goat serum in phosphate-buffered saline (PBS)) on a clean parafilm sheet and incubated for 45 min at room temperature. Cells were then incubated in PBS with rabbit anti-SIRT1 (1:100) or rabbit anti-SIRT7 (1:100) and mouse anti-Flag (1:1000) for 1 h at room temperature. After washing with PBS, coverslips were incubated with Alexa Fluor 488-conjugated goat anti-rabbit IgG (1: 5000; Molecular Probes, Waltham, MA, USA) for 1 h in the dark at room temperature. Coverslips were additionally incubated with DAPI (4',6-diamidino-2-phenylindole) for 20 min at room temperature to stain nuclear DNA. Images were acquired using a Nikon Eclipse Ti microscope (Nikon Americas Inc., Melville, NY, USA).

Real-time PCR

RNA was extracted by using the TRI reagent (Thermo Fisher Scientific, Waltham, MA, USA). cDNA was generated by using the RNA Reverse Transcription Kit (Applied Biosystems, Warrington, UK). Quantitative reverse transcription–PCR (RT–PCR) was performed in a CFX96 Real-Time System (Bio-Rad, Hercules, CA, USA) using specific sense and antisense primers in 25 μl reaction volumes containing 12.5 μl SYBR Green PCR Master Mix (Applied Biosystems), 10.5 μl of 1 μmol/l primer stock and 2 μl of cDNA (1:10 diluted). Primer sequences are presented in Table 2.

Western blots

Whole-cell lysates were prepared from cells that had been washed and harvested by centrifugation in PBS. Cell pellets were resuspended in RIPA buffer that contained 50 mM Tris, pH 7.5, 150 mM sodium chloride, 1% NP-40, 0.2% sodium dodecyl sulfate, 0.5% sodium deoxycholate, 0.1 mM EDTA and 1% protease and phosphatase inhibitors (Sigma-Aldrich). Lysates were centrifuged and supernatants were collected. Cell lysates (25 μg) were separated by 10% sodium dodecyl sulfate–polyacrylamide gel electrophoresis and transferred to polyvinylidene difluoride membranes (Immobilon-P membranes; Millipore, Billerica, MA, USA). Membranes were blocked with blocking buffer (5% skim milk, 0.1% Tween-20 in PBS) for 1 h at room temperature. After incubation with primary antibodies overnight at 4 °C, membranes were then incubated with horseradish peroxidase-conjugated secondary antibodies, detected using the ECL Plus Western Blotting Detection System (Amersham Biosciences, Piscataway, NJ, USA) with the ODYSSEY Fc, Dual-Mode Imaging System (Li-COR, Lincoln, NE, USA).

Measurements of SIRT activity and NAD^+ concentration in cells

SIRT activity was determined with a fluorometric kit purchased from Sigma-Aldrich (CS1040) used according to the manufacturer's instructions, with minor modifications. Cells were lysed in RIPA buffer containing Trichostatin A (TSA, 5 μM, Sigma-Aldrich) to block histone deacetylase activity and then incubated for 10 min at 37 °C to allow degradation of any contaminant NAD^+. Extracts (30 μg protein per reaction) were then incubated with 10 μl SIRT substrate solution in the presence or absence of NAD^+. Plates were incubated at 37 °C

for 1 h, 5 μl of developing buffer was added to each well and plates were incubated at 37 °C for 10 min. Fluorescence intensity (excitation wavelength = 360 nm, emission wavelength = 450 nm) was measured using a FLUOstar Omega Plate Reader (BMG Labtech, Ortenberg, Germany). The SIRT inhibitor nicotinamide was used to confirm the specificity of the reaction; the fluorescence values obtained in the absence of NAD^+ did not differ from the blank. SIRT-dependent deacetylase activity was calculated after subtracting fluorescence values obtained in the absence of NAD^+. In all cases, we confirmed the linearity of the reaction over time.

NAD^+ concentration was determined by using the NAD/NADH Cell Based Assay Kit (Cayman Chemical) according to the manufacturer's instructions. Briefly, THP-1 cells were washed with ice-cold PBS and lysed with a permeabilization buffer at room temperature for 30 min. Cell lysates were centrifuged at 1000 *g* for 10 min, supernatants were transferred to 96-well plates and 100 μl reaction buffer were added to each well. After incubating at room temperature for 1.5 h on a plate shaker, the absorbance of each well was measured by FLUOstar Omega at 450 nm.

Immunoprecipitation

HeLa cells were seeded at 4×10^6 cells per 10 cm plate and were transiently transfected with 8 μg of pCDNA3 Flag MKK7B2Jnk1a1, pCDNA3 Flag p38α, pFLAG-CMV-hErk1 or p3xFlag-CMV7-Erk2 and co-transfected with wild-type HA-FOXO3 or various FOXO3 mutant constructs. One day after transfection, cells were incubated in the presence of TSA (10 μM), sirtinol (Sigma-Aldrich; 20 μM), RSV (100 μM) or TSA plus sirtinol for 2 h before harvest and were then lysed in the lysis buffer described above. For each immunoprecipitation experiment, 400 μg cell extracts were subjected to immunoprecipitation with 50 μl anti-Flag M2 magnetic beads (Sigma-Aldrich) or 50 μl anti-HA magnetic beads (Thermo Fisher Scientific). The immune complexes were analyzed by western blot.

in vitro deacetylation assay

HeLa cells were seeded at 4×10^6 cells per 10 cm and cultured overnight. Thereafter, cells were incubated in the absence or in the presence of hydrogen peroxidase (400 μM, 1 h). Extracts were obtained by lysing the cells in RIPA buffer as above. Cell extracts were subjected to immunoprecipitation using FOXO3 antibody (75D8). Purified FOXO3 was incubated in histone deacetylase buffer (10 mM Tris-HCl, pH 8.0, 150 mM NaCl, 10% glycerol) with purified recombinant human SIRT7 (0.4 μg), in the presence or absence of NAD^+ (60 μM) for 1 h at 30 °C. The reactions were resolved on sodium dodecyl sulfate–polyacrylamide gel electrophoresis and analyzed by western blot.

Acetylation of endogenous FOXO3

THP-1 cells transfected with siSIRT7 described above were seeded at 7.5×10^5 cells per T25 flask. After 3 days, cells were incubated in the presence of TSA (5 μM) for 2 h. Cells were lysed in the lysis buffer described above. Total cell extracts (400 μg protein) were subjected to immunoprecipitation with 4 μg rabbit polyclonal antibody to FOXO3. The immune complexes were analyzed by western blotting with anti-acetyl-K antibody.

Caspase-3/7 activity and TUNEL assay

Caspase-3/7 activity was determined using the Caspase-Glo 3/7 Assay System (Promega, Madison, WI, USA) according to the manufacturer's instructions. For TUNEL assays, cells were fixed with 4% paraformaldehyde at room temperature for 10 min. After a PBS rinse, cells were stained using the DeadEND Fluorometric TUNEL System (Promega) according to the manufacturer's instructions. Quantification of TUNEL staining was performed by examining at least five randomly selected fields.

Human primary monocyte isolation

Blood was collected from HCs and AH patients. Inclusion criteria for AH subjects were as follows: age 18–70 years, both genders, currently hospitalized with a diagnosis of AH. For HCs: age 18–70 years, both genders, no history of liver disease, no alcohol consumption for 72 h before collection. All human tissues were obtained with individual informed consent and the study was approved by the Institutional Review Board at the University of Kansas Medical Center. Isolation of peripheral blood mononuclear cells from human blood was performed by density gradient centrifugation. Briefly, whole blood was centrifuged for 15 min at 1180 *g* with no brake. Buffy coats were collected and resuspended in PBS (1:1), layered over Histopaque 1077 (Sigma-Aldrich) and centrifuged for 45 min at 250 *g* with no brake. The peripheral blood mononuclear cell fraction was washed two times with PBS and resuspended in MACS buffer (0.5% fetal bovine serum, 2 mM EDTA in PBS). Monocytes were isolated by positive selection using magnetic CD14 microbeads (human; cat. no. 130-050-201; Miltenyi Biotech, Auburn, CA, USA) according to the manufacturer's instructions.

Statistical analysis

For cell culture experiments, each experiment was repeated at least three times with two technical replicates each unless indicated otherwise, as this was generally sufficient to achieve statistical significance for differences. Sample sizes for individual experiments are specified in figure legends. For human sample experiments, we had no *a priori* information on effect magnitude or standard deviation, thus sample sizes (control = 12; alcoholic hepatitis = 18) were chosen based on subject to availability. These numbers were sufficient to achieve statistical significance for multiple measures. Data are presented as mean ± s.d. Statistical significance between groups was calculated by using one-way analysis of variance, followed by Turkey's test. Statistical significance between the two groups was calculated by two-tailed unpaired Student's *t*-test. Variance between groups met the assumptions or the appropriate test. Unless otherwise stated, a *P*-value of < 0.05 was considered statistically significant.

ACKNOWLEDGEMENTS

This study was supported by grant AA012863 from the National Institute on Alcoholism and Alcohol Abuse, a fellowship grant from the Biomedical Research Training Program of the University of Kansas Medical Center (to ZL) and by a grant from the Hubert and Richard Hanlon Trust. The human monocytes used in this study were provided by the University of Kansas Liver Center Tissue Bank. We thank Drs Charles Rice and Robert A Davey for providing reagents for these studies.

REFERENCES

1. Dijkers PF, Medema RH, Pals C, Banerji L, Thomas NS, Lam EW, et al. Forkhead transcription factor FKHR-L1 modulates cytokine-dependent transcriptional regulation of p27(KIP1). Mol Cell Biol. 2000; 20:9138–9148. [PubMed: 11094066]
2. Tran H, Brunet A, Grenier JM, Datta SR, Fornace AJ Jr, DiStefano PS, et al. DNA repair pathway stimulated by the forkhead transcription factor FOXO3a through the Gadd45 protein. Science. 2002; 296:530–534. [PubMed: 11964479]
3. Chung YW, Kim HK, Kim IY, Yim MB, Chock PB. Dual function of protein kinase C (PKC) in 12-O-tetradecanoylphorbol-13-acetate (TPA)-induced manganese superoxide dismutase (MnSOD) expression: activation of CREB and FOXO3a by PKC-alpha phosphorylation and by PKC-mediated inactivation of Akt, respectively. J Biol Chem. 2011; 286:29681–29690. [PubMed: 21705328]
4. Hagenbuchner J, Kuznetsov A, Hermann M, Hausott B, Obexer P, Ausserlechner MJ. FOXO3-induced reactive oxygen species are regulated by BCL2L11 (Bim) and SESN3. J Cell Sci. 2012; 125:1191–1203. [PubMed: 22349704]
5. Ni HM, Du K, You M, Ding WX. Critical role of FoxO3a in alcohol-induced autophagy and hepatotoxicity. Am J Pathol. 2013; 183:1815–1825. [PubMed: 24095927]
6. Calnan DR, Brunet A. The FoxO code. Oncogene. 2008; 27:2276–2288. [PubMed: 18391970]
7. Miyamoto K, Araki KY, Naka K, Arai F, Takubo K, Yamazaki S, et al. Foxo3a is essential for maintenance of the hematopoietic stem cell pool. Cell Stem Cell. 2007; 1:101–112. [PubMed: 18371339]
8. Su JL, Cheng X, Yamaguchi H, Chang YW, Hou CF, Lee DF, et al. FOXO3a-dependent mechanism of E1A-induced chemosensitization. Cancer Res. 2011; 71:6878–6887. [PubMed: 21911455]
9. Yang JY, Zong CS, Xia W, Yamaguchi H, Ding Q, Xie X, et al. ERK promotes tumorigenesis by inhibiting FOXO3a via MDM2-mediated degradation. Nat Cell Biol. 2008; 10:138–148. [PubMed: 18204439]
10. Zou Y, Tsai WB, Cheng CJ, Hsu C, Chung YM, Li PC, et al. Forkhead box transcription factor FOXO3a suppresses estrogen-dependent breast cancer cell proliferation and tumorigenesis. Breast Cancer Res. 2008; 10:R21. [PubMed: 18312651]
11. Fu Z, Tindall DJ. FOXOs, cancer and regulation of apoptosis. Oncogene. 2008; 27:2312–2319. [PubMed: 18391973]
12. Li Z, Zhao J, Tikhanovich I, Kuravi S, Helzberg J, Dorko K, et al. Serine 574 phosphorylation alters transcriptional programming of FOXO3 by selectively enhancing apoptotic gene expression. Cell Death Differ. 2015; 23:583–595. [PubMed: 26470730]
13. Brunet A, Sweeney LB, Sturgill JF, Chua KF, Greer PL, Lin Y, et al. Stress-dependent regulation of FOXO transcription factors by the SIRT1 deacetylase. Science. 2004; 303:2011–2015. [PubMed: 14976264]
14. North BJ, Verdin E. Sirtuins: Sir2-related NAD-dependent protein deacetylases. Genome Biol. 2004; 5:224. [PubMed: 15128440]
15. Canto C, Gerhart-Hines Z, Feige JN, Lagouge M, Noriega L, Milne JC, et al. AMPK regulates energy expenditure by modulating NAD+ metabolism and SIRT1 activity. Nature. 2009; 458:1056–1060. [PubMed: 19262508]
16. Satoh A, Brace CS, Rensing N, Cliften P, Wozniak DF, Herzog ED, et al. Sirt1 extends life span and delays aging in mice through the regulation of Nk2 homeobox 1 in the DMH and LH. Cell Metab. 2013; 18:416–430. [PubMed: 24011076]
17. Tseng AH, Shieh SS, Wang DL. SIRT3 deacetylates FOXO3 to protect mitochondria against oxidative damage. Free Radic Biol Med. 2013; 63:222–234. [PubMed: 23665396]
18. Wang Y, Zhu Y, Xing S, Ma P, Lin D. SIRT5 prevents cigarette smoke extract-induced apoptosis in lung epithelial cells via deacetylation of FOXO3. Cell Stress Chaperones. 2015; 20:805–810. [PubMed: 25981116]
19. Simic P, Zainabadi K, Bell E, Sykes DB, Saez B, Lotinun S, et al. SIRT1 regulates differentiation of mesenchymal stem cells by deacetylating beta-catenin. EMBO Mol Med. 2013; 5:430–440. [PubMed: 23364955]

20. Jeong J, Juhn K, Lee H, Kim SH, Min BH, Lee KM, et al. SIRT1 promotes DNA repair activity and deacetylation of Ku70. Exp Mol Med. 2007; 39:8–13. [PubMed: 17334224]
21. Ponugoti B, Kim DH, Xiao Z, Smith Z, Miao J, Zang M, et al. SIRT1 deacetylates and inhibits SREBP-1C activity in regulation of hepatic lipid metabolism. J Biol Chem. 2010; 285:33959–33970. [PubMed: 20817729]
22. Wang F, Nguyen M, Qin FX, Tong Q. SIRT2 deacetylates FOXO3a in response to oxidative stress and caloric restriction. Aging Cell. 2007; 6:505–514. [PubMed: 17521387]
23. Jin YH, Kim YJ, Kim DW, Baek KH, Kang BY, Yeo CY, et al. Sirt2 interacts with 14-3-3 beta/gamma and down-regulates the activity of p53. Biochem Biophys Res Commun. 2008; 368:690–695. [PubMed: 18249187]
24. Rothgiesser KM, Erener S, Waibel S, Luscher B, Hottiger MO. SIRT2 regulates NF-kappaB dependent gene expression through deacetylation of p65 Lys310. J Cell Sci. 2010; 123:4251–4258. [PubMed: 21081649]
25. Vaziri H, Dessain SK, Ng Eaton E, Imai SI, Frye RA, Pandita TK, et al. hSIR2(SIRT1) functions as an NAD-dependent p53 deacetylase. Cell. 2001; 107:149–159. [PubMed: 11672523]
26. Liu Y, Shepherd EG, Nelin LD. MAPK phosphatases—regulating the immune response. Nat Rev Immunol. 2007; 7:202–212. [PubMed: 17318231]
27. Nasrin N, Kaushik VK, Fortier E, Wall D, Pearson KJ, de Cabo R, et al. JNK1 phosphorylates SIRT1 and promotes its enzymatic activity. PLoS One. 2009; 4:e8414. [PubMed: 20027304]
28. Wang F, Chan CH, Chen K, Guan X, Lin HK, Tong Q. Deacetylation of FOXO3 by SIRT1 or SIRT2 leads to Skp2-mediated FOXO3 ubiquitination and degradation. Oncogene. 2012; 31:1546–1557. [PubMed: 21841822]
29. Grozinger CM, Chao ED, Blackwell HE, Moazed D, Schreiber SL. Identification of a class of small molecule inhibitors of the sirtuin family of NAD-dependent deacetylases by phenotypic screening. J Biol Chem. 2001; 276:38837–38843. [PubMed: 11483616]
30. McKeever UM, O'Mahoney C, Lawlor E, Kinsella A, Weir DG, Feighery CF. Monocytosis: a feature of alcoholic liver disease. Lancet. 1983; 2:1492. [PubMed: 6140576]
31. Khongkow M, Olmos Y, Gong C, Gomes AR, Monteiro LJ, Yague E, et al. SIRT6 modulates paclitaxel and epirubicin resistance and survival in breast cancer. Carcinogenesis. 2013; 34:1476–1486. [PubMed: 23514751]
32. Flick F, Luscher B. Regulation of sirtuin function by posttranslational modifications. Front Pharmacol. 2012; 3:29. [PubMed: 22403547]
33. Caito S, Rajendrasozhan S, Cook S, Chung S, Yao H, Friedman AE, et al. SIRT1 is a redox-sensitive deacetylase that is post-translationally modified by oxidants and carbonyl stress. FASEB J. 2010; 24:3145–3159. [PubMed: 20385619]
34. Olsen JV, Blagoev B, Gnad F, Macek B, Kumar C, Mortensen P, et al. Global, *in vivo*, and site-specific phosphorylation dynamics in signaling networks. Cell. 2006; 127:635–648. [PubMed: 17081983]
35. Sasaki T, Maier B, Koclega KD, Chruszcz M, Gluba W, Stukenberg PT, et al. Phosphorylation regulates SIRT1 function. PLoS One. 2008; 3:e4020. [PubMed: 19107194]
36. Zschoernig B, Mahlknecht U. Carboxy-terminal phosphorylation of SIRT1 by protein kinase CK2. Biochem Biophys Res Commun. 2009; 381:372–377. [PubMed: 19236849]
37. Gao Z, Zhang J, Kheterpal I, Kennedy N, Davis RJ, Ye J. Sirtuin 1 (SIRT1) protein degradation in response to persistent c-Jun N-terminal kinase 1 (JNK1) activation contributes to hepatic steatosis in obesity. J Biol Chem. 2011; 286:22227–22234. [PubMed: 21540183]
38. Elmali N, Baysal O, Harma A, Esenkaya I, Mizrak B. Effects of resveratrol in inflammatory arthritis. Inflammation. 2007; 30:1–6. [PubMed: 17115116]
39. Lee SM, Yang H, Tartar DM, Gao B, Luo X, Ye SQ, et al. Prevention and treatment of diabetes with resveratrol in a non-obese mouse model of type 1 diabetes. Diabetologia. 2011; 54:1136–1146. [PubMed: 21340626]
40. Lucey MR, Mathurin P, Morgan TR. Alcoholic hepatitis. N Engl J Med. 2009; 360:2758–2769. [PubMed: 19553649]

41. Roychowdhury S, McMullen MR, Pritchard MT, Hise AG, van Rooijen N, Medof ME, et al. An early complement-dependent and TLR-4-independent phase in the pathogenesis of ethanol-induced liver injury in mice. Hepatology. 2009; 49:1326–1334. [PubMed: 19133650]

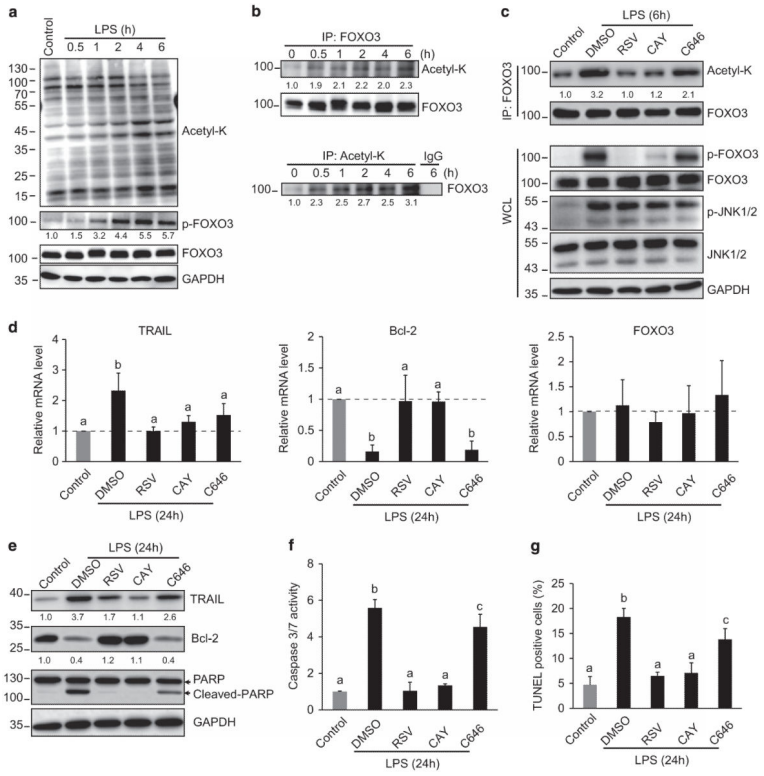

Figure 1.

Acetylation of FOXO3 is essential for p-FOXO3 formation and apoptosis after LPS. (**a**) THP-1 cells were treated with 100 ng/ml LPS for 6 h and harvested at various times as indicated. p-FOXO3 and acetylation of FOXO3 were analyzed by western blot. Data are representative of three independent experiments. The numbers below the lanes indicate relative p-FOXO3 protein level normalized to glyceraldehyde 3-phosphate dehydrogenase (GAPDH). (**b**) Immunoprecipitation (IP) analysis of acetylation status of FOXO3 after 100 ng/ml LPS treatment at times indicated. Data are representative of three independent experiments; numbers below the lanes indicate relative acetyl-K band intensity. (**c**) THP-1 cells were pretreated with dimethyl sulfoxide (DMSO), RSV (100 μM), CAY10591 (CAY, 50 μM) or C646 (25 μM) for 4 h and then treated with 100 ng/ml LPS for 6 h. Upper panel: IP experiment to access acetylation status of FOXO3. Lower panel: Western blot of whole-cell lysis (WCL) from these same cells. Data are representative of three independent experiments. (**d**) Real-time RT–PCR analysis of Bcl-2, TRAIL and FOXO3 mRNA levels in THP-1 cells pretreated with DMSO, RSV, CAY or C646 for 4 h and then treated with 100 ng/ml LPS for 24 h. (**e–g**) Protein expression (**e**), caspase-3/7 activity (**f**) and TUNEL assay (**g**) in these same cells 24 h after LPS treatment. Graphs show mean ± s.d. of three independent experiments with technical duplicates. The number below the lanes indicate relative band intensity normalized to GAPDH. Values with different superscripts are significantly different from each other ($P < 0.05$, one-way analysis of variance (ANOVA)).

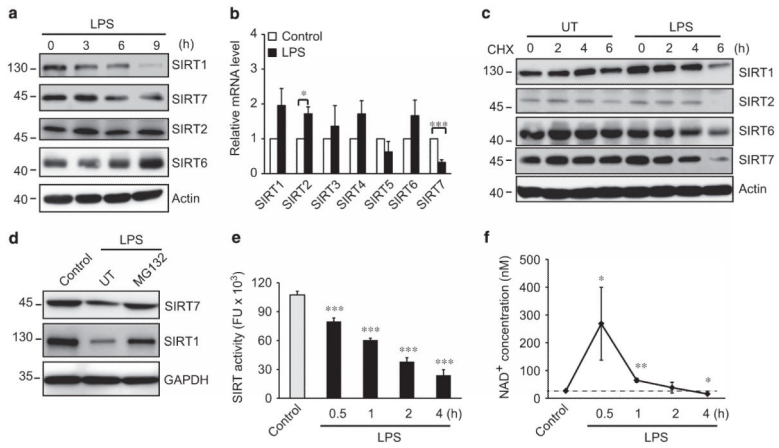

Figure 2.

LPS induces downregulation of SIRT activity by targeting SIRT1 and SIRT7 proteins for degradation. (**a**) SIRT protein levels in THP-1 cells treated with 100 ng/ml LPS for times indicated. Data are representative of three independent experiments. (**b**) Real-time RT–PCR analysis of SIRTs family mRNA levels in THP-1 cells treated with 100 ng/ml LPS for 24 h. Data represent mean ± s.d. of three independent experiments with technical duplicates. (**c**) SIRT protein half-life in THP-1 cells either untreated (UT) or treated with 100 ng/ml LPS for indicated times in the presence of cycloheximide (CHX, 100 μM). Data are representative of three independent experiments. (**d**) SIRT1 and SIRT7 protein levels in THP-1 cells either untreated (control) or treated with 100 ng/ml LPS for 6 h in the absence (UT) or presence of the proteasome inhibitor MG-132 (50 μM). Data are representative of three independent experiments. (**e** and **f**) SIRT activity and NAD^+ concentration in cells either untreated (control) or treated with 100 ng/ml LPS for various times as indicated. Data represent mean ± s.d. of three independent experiments. $*P < 0.05$, $**P < 0.01$ and $***P < 0.01$ compared with control, Student's *t*-test.

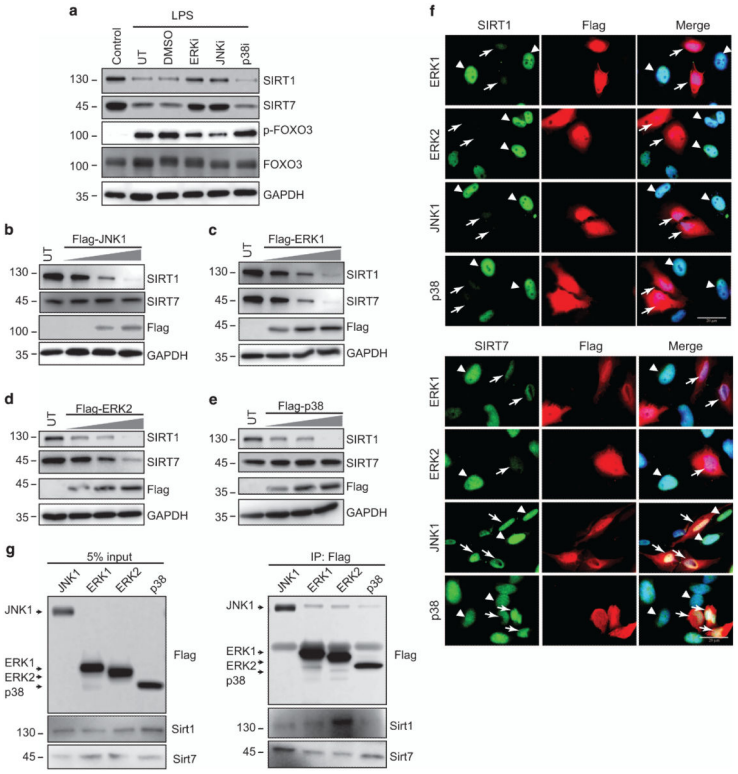

Figure 3.

MAPK dependence of SIRT1 and SIRT7 protein degradation. (**a**) THP-1 cells without (control) or with treatment with 100 ng/ml LPS for 6 h in the absence (UT) or presence of dimethyl sulfoxide (DMSO), ERK inhibitor (ERKi, 5 μM), JNK inhibitor (JNKi, 50 μM) or p38 inhibitor (p38i, 50 μM). Protein levels of SIRT1, SIRT7 and p-FOXO3 were evaluated by western blot. Data are representative of three independent experiments. (**b–f**) HeLa cells were either untransfected (UT) or transfected with increasing amount of Flag-tagged ERK1, ERK2, JNK1 or p38 plasmids for 24 h, after which SIRT1 and SIRT7 protein levels were evaluated by western blot (**b–e**) or immunofluorescence with SIRT1 or SIRT7 (green) and Flag antibodies (red) (**f**). Data are representative of three independent experiments. Arrows indicate transfected cells and arrowheads indicate untransfected cells. Scale bar indicates 20 μm. (**g**) HeLa cells were transfected with Flag-tagged ERK1, ERK2, JNK1 or p38 plasmid for 24 h and cell extracts were subjected to immunoprecipitation with magnetic beads to Flag, immune complexes were analyzed by western blot with antibody to SIRT1 or SIRT7. Data are representative of three independent experiments.

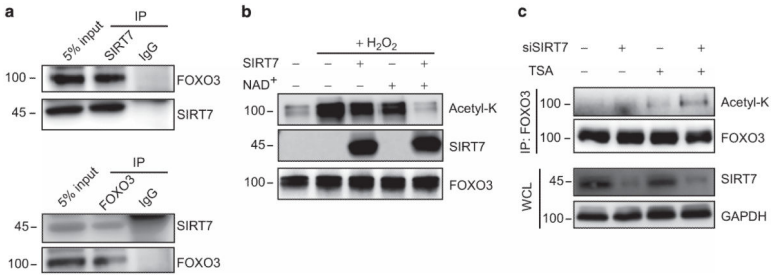

Figure 4.

SIRT7 deacetylates FOXO3 *in vitro* and *in vivo*. (**a**) Interaction of endogenous SIRT7 and FOXO3. Endogenous SIRT7 or FOXO3 were immunoprecipitated from THP-1 cell lysates and the both input and immune complexes were assessed for the presence of FOXO3 or SIRT7 by western blot. Data are representative of three independent experiments. (**b**) Deacetylation of FOXO3 by SIRT7 *in vitro*. The HA-tagged form of FOXO3 was purified from HeLa cells treated with or without hydrogen peroxidase (H_2O_2) (400 μM, 1 h). Purified FOXO3 was incubated in the presence or absence of rSIRT7 with or without NAD^+. Acetylated FOXO3 and total amount of FOXO3 were assessed by western blot with anti-acetyl-K and FOXO3. Data are representative of four independent experiments. (c) Deacetylation of FOXO3 by SIRT7 in cells. THP-1 cells were transfected with siSIRT7 for 72 h and then incubated in the presence of TSA (5 μM) for 2 h. Cells were lysed and cell extracts were subjected to immunoprecipitation with antibody to FOXO3. Acetylated FOXO3 was analyzed by western blot with anti-acetyl-K and total protein was evaluated in whole-cell lysates (WCL) by western blot. Data are representative of three independent experiments.

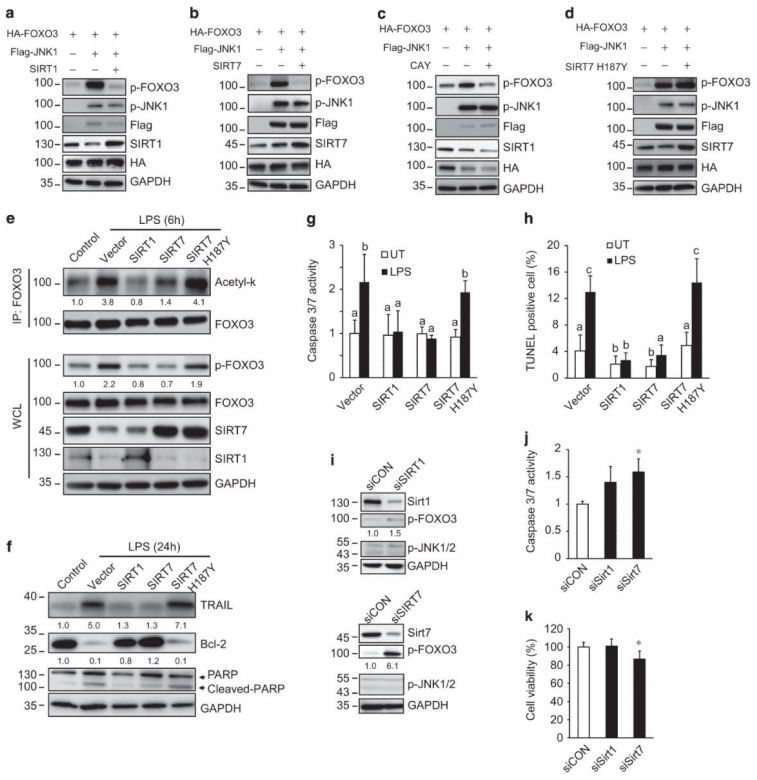

Figure 5.

SIRT1 and SIRT7 direct p-FOXO3 formation and apoptosis. (**a–d**) HA-FOXO3 and Flag-JNK1 were co-transfected with SIRT1, SIRT7, SIRT7 H187Y or treated with SIIRT1 activator (CAY, 50 μM) in HeLa cells. SIRT1, SIRT7 and p-FOXO3 protein levels were evaluated by western blot 24 h after transfection. Data are representative of three independent experiments. (**e–h**) THP-1 cells were electroporated with empty vector (EV), Flag-SIRT1, Flag-SIRT7 or Flag-SIRT7 H187Y for 48 h. Thereafter, cells received either no treatment (UT) or treatment with 100 ng/ml LPS for 6 h. FOXO3 acetylation was assessed by IP and SIRT1, SIRT7 and p-FOXO3 protein levels were evaluated by western blot in whole-cell lysates. The number below the lanes indicate relative band intensity (**e**). Bcl-2, TRAIL and poly (ADP-ribose) polymerase (PARP) protein levels, caspase-3/7 activity and TUNEL assay and were measured 24 h after LPS (**f–h**). Graphs show mean ± s.d. of three independent experiments. Values with different superscripts are significantly different from each other ($P < 0.05$, one-way analysis of variance (ANOVA)). (**i–k**) THP-1 cells were transfected with siRNA specific for SIRT1 or SIRT7 (siSIRT1, siSIRT7) or non-targeting control vectors (siCON) for 72 h. SIRT1, SIRT7 and p-FOXO3 protein levels were evaluated by western blot (**i**). Data are representative of three independent experiments. The number below the lanes indicate relative band intensity. Caspase-3/7 activity (**j**) and cell viability (**k**) were also performed to evaluate cell death. Graphs show mean ± s.d. of three independent experiments. *$P < 0.05$ compare to siCON, Student's *t*-test.

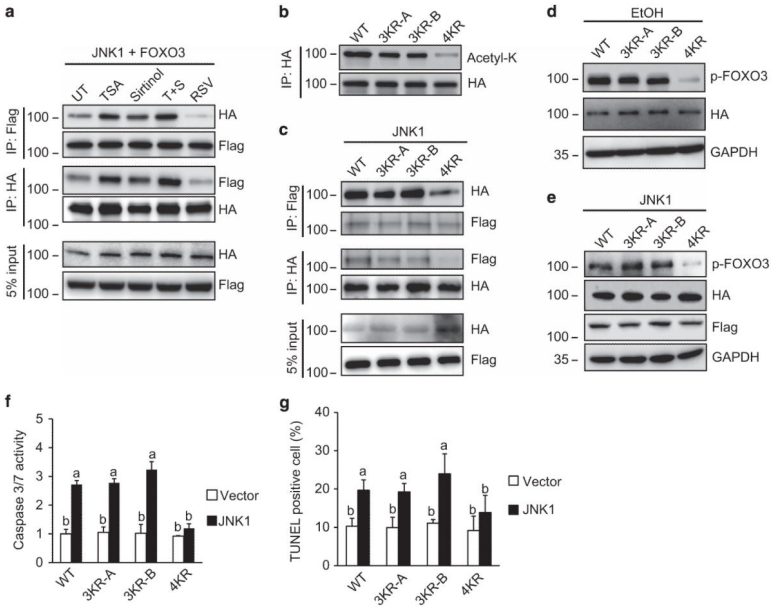

Figure 6.

Acetylated FOXO3 binds preferentially to JNK1. (a) HeLa cells were transfected with Flag-JNK1 and HA-FOXO3 for 24 h and treated with TSA (10 μM), sirtinol (20 μM), TSA plus sirtinol or RSV (100 μM) for 2 h. Cells were lysed and cell extracts were subjected to immunoprecipitation with magnetic beads for HA or Flag; the immune complexes were then assessed for the presence of Flag-JNK1 or HA-FOXO3 by western blot. Data are representative of three independent experiments. (**b**) Acetylation of FOXO3 mutants. HeLa cells were co-transfected with Flag-JNK1 with wild-type (wt) HA-FOXO3, HA-FOXO3-3KR-A (K242R, K259R and K290R), HA-FOXO3-3KR-B (K242R, K259R and K569R) or HA-FOXO3-4KR (K242R, K259R, K290R and K569R) for 24 h; cells were lysed and cell extracts were subjected to immunoprecipitation with magnetic beads for HA. Acetylated FOXO3 was analyzed by western blot with anti-acetyl-K. Total amounts of FOXO3 were assessed by western blot with HA antibody. Data are representative of three independent experiments. (**c**) Interaction of HA-FOXO3 and FOXO3 KR mutant were assessed as in (**a**). (**d**) Huh7.5 cells were transfected with HA-FOXO3 or FOXO3 mutants overnight and then treated with 50 mM EtOH for an additional 24 h; p-FOXO3 was assessed by western blot. Data are representative of three independent experiments. (**e–g**) HeLa cells were co-transfected with Flag-JNK1 with wt-FOXO3 or FOXO3 mutants for 24 h, p-FOXO3 was assessed by western blot (**e**) and caspase-3/7 activity (**f**) and cell death assessed by TUNEL assay (**g**) were measured. Data are representative of three independent experiments. Graphs show mean ± s.d. of three independent experiments. Values with different superscripts are significantly different from each other ($P < 0.01$, one-way analysis of variance (ANOVA)).

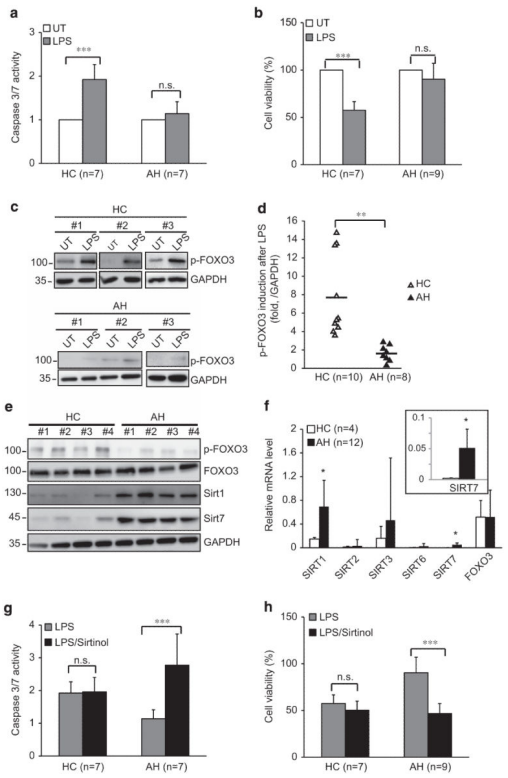

Figure 7.

Defects of p-FOXO3 formation and apoptosis in blood monocytes from patients with AH. (**a** and **b**) Isolated monocytes from HC ($n = 7$) or AH patients (AH, $n = 8 \sim 10$) were either left untreated (UT) or treated with 100 ng/ml LPS for 24 h. Cell death was evaluated by capase-3/7 activity (**a**) and cell viability (**b**). (**c**) Representative western blots from isolated monocytes either untreated (UT) or treated with 100 ng/ml LPS for 6 h. (**d**) p-FOXO3 induction in isolated monocytes from HC ($n = 10$) and AH ($n = 8$) after LPS treatment. The data are presented as fold increase after LPS treatment and was normalized to glyceraldehyde 3-phosphate dehydrogenase (GAPDH). Line represents the mean value. (**e**) SIRT1, SIRT7 and p-FOXO3 levels in isolated monocytes from HC and AH patients. Each lane represents a cell lysis from a single individual. (**f**) Real-time RT–PCR analysis of SIRT family mRNA levels in isolated monocytes from HC ($n = 4$) or AH patients ($n = 12$). The inset shows an enlarged graph of SIRT7 mRNA level. (**g** and **h**) Isolated monocytes from HC or AH mentioned above were either left untreated (UT) or treated with 100 ng/ml LPS in the absence or presence of sirtinol (50 μM) for 24 h; cell death was evaluated by capase-3/7 activity (**g**) and cell viability (**h**) compared with untreated cells. Graphs show mean ± s.d. $*P<0.05$, $***P<0.001$ and NS, not significant, Student's *t*-test.

Table 1

Characteristics of alcoholic hepatitis patients

	***Alcoholic hepatitis* (n=*18*)**			***Healthy control*[a] (n=*12*)**		
	Range	***Mean***	**%**	***Range***	***Mean***	**%**
Age	27–62	47		29–59	37	
Sex (F)			42			33
ALT (U/l)	17–149	51		ND		
AST (U/l)	19–419	126		ND		
Total bilirubin (mg/dl)	0.2–36.9	14.6		ND		
Albumin (mg/dl)	2.5–3.9	3.2		ND		

Abbreviations: ALT, alanine transaminase; AST, aspartate transaminase; ND, not determined.

[a]No alcohol consumption for at least 72 h before sample collection.

Table 2

Primer sequences used for RT-PCR

TRAIL forward	5'-GACCTGCGTGCTGATCGTG-3'
TRAIL reverse	5'-TGTCCTGCATCTGCTTCAGCT-3'
F0X03 forward	5'-GGGGAACTTCACTGGTGCTA-3'
FOX03 reverse	5'-TGTCCACTTGCTGAGAGCAG-3'
Bcl-2 forward	5'-TTTTAGGAGACCGAAGTCCG-3'
Bcl-2 reverse	5'-AGCCAACGTGCCATGTGCTA-3'
SIRT1 forward	5'-TAGCCTTGTCAGATAAGGAAGGA-3'
SIRT1 reverse	5'-ACAGCTTCACAGTCAACTTTGT-3'
SIRT2 forward	5'-TGCGGAACTTATTCTCCCAGA-3'
SIRT2 reverse	5'-GAGAGCGAAAGTCGGGGAT-3'
SIRT3 forward	5'-ACCCAGTGGCATTCCAGAC-3'
SIRT3 reverse	5'-GGCTTGGGGTTGTGAAAGAAG-3'
SIRT4 forward	5'-GCTTTGCGTTGACTTTCAGGT-3'
SIRT4 reverse	5'-CCAATGGAGGCTTTCGAGCA-3'
SIRT5 forward	5'-GCCATAGCCGAGTGTGAGAC-3'
SIRT5 reverse	5'-CAACTCCACAAGAGGTACATCG-3'
SIRT6 forward	5'-CCCACGGAGTCTGGACCAT-3'
SIRT6 reverse	5'-CTCTGCCAGTTTGTCCCTG-3'
SIRT7 forward	5'-GACCTGGTAACGGAGCTGC-3'
SIRT7 reverse	5'-CGACCAAGTATTTGGCGTTCC-3'
GAPDH forward	5'-GAAGGTGAAGGTCGGAGTC-3'
GAPDH reverse	5'-GAAGATGGTGATGGGATTTC-3'

Abbreviations: GAPDH, glyceraldehyde 3-phosphate dehydrogenase; RT-PCR, reverse transcription-PCR; SIRT, sirtuin; TRAIL, tumor necrosis factor-related apoptosis-inducing ligand.